

See discussions, stats, and author profiles for this publication at: <https://www.researchgate.net/publication/231645616>

Interface Water on TiO₂ Anatase (101) and (001) Surfaces: First-Principles Study with TiO₂ Slabs Dipped in Bulk Water

ARTICLE *in* THE JOURNAL OF PHYSICAL CHEMISTRY C · OCTOBER 2010

Impact Factor: 4.77 · DOI: 10.1021/jp105364z

CITATIONS

44

READS

59

3 AUTHORS, INCLUDING:



Masato Sumita

National Institute for Materials Science

35 PUBLICATIONS 312 CITATIONS

[SEE PROFILE](#)



Chunping Hu

Tokyo University of Science

32 PUBLICATIONS 409 CITATIONS

[SEE PROFILE](#)

Interface Water on TiO₂ Anatase (101) and (001) Surfaces: First-Principles Study with TiO₂ Slabs Dipped in Bulk Water

Masato Sumita,[†] Chunping Hu,^{†,§} and Yoshitaka Tateyama*,^{†,‡}

International Center for Materials Nanoarchitectonics (MANA) and Innovation Center of Nanomaterials Science for Environment and Energy, National Institute for Materials Science (NIMS), 1-1 Namiki, Tsukuba, Ibaraki 305-0044, Japan PRESTO and CREST, Japan Science and Technology Agency, 4-1-8 Honcho, Kawaguchi, Saitama 333-0012, Japan

Received: June 11, 2010; Revised Manuscript Received: September 14, 2010

We investigated the TiO₂ anatase (101) and (001) interfaces dipped in bulk water on the atomic scale by first-principles density-functional molecular dynamics simulations. We verified that the water adsorption models proposed in the previous studies with less than a couple of water layers on the vacuum surfaces still hold. On the contrary, novel adsorption structures of interfacial water molecules are also found. Our results indicate that water molecules around the interface between the TiO₂ and bulk water can be described by the following two-layer model: The first water layer can be defined as the water molecules adsorbed at Ti_{5c} sites molecularly on the anatase (101) surfaces and dissociatively on the (001). The second layer on the anatase (101) surface can be defined as the water molecules adsorbed to O_{2c} or adsorbed water to Ti_{5c} via strong HB. Second layer on the (001) consists of water molecules bound to the first-layer water molecules via the strong and weak HBs. Contour maps of the atomic densities show that water molecules in the second layers are relatively mobile. This two-layer model well accounts for the experimental results of solid-state ¹H NMR.

1. Introduction

TiO₂ is a most important photocatalyst,¹ widely used in many applications with an aqueous environment. However, the atomistic mechanisms of catalytic reactions on the TiO₂/water interfaces have not been fully understood yet. For this issue, many studies on bare TiO₂ surfaces with adsorption of some water molecules have been carried out theoretically and experimentally, and their results give several insights into structures and electronic states for the TiO₂/water interfaces.^{2–10} Even so it is still essential to elucidate behavior of water molecules on the TiO₂/water interfaces in the real working conditions (i.e., aqueous environment). To this end, we have carried out first-principles molecular dynamics simulations using supercells involving TiO₂ slab and bulk water in this study. Note that TiO₂ has two representative polymorphs, rutile and anatase, and in general the anatase (101) surface is regarded to be most relevant to catalytic reactivity of TiO₂. Therefore, we focus on the TiO₂ anatase polymorphs in this study.

The adsorption feature of water molecules on bare surfaces of TiO₂ anatase polymorph in vacuo was first proposed by first-principles calculations.^{6a} The results showed that molecular adsorption at the 5-fold coordinated Ti (Ti_{5c}) site is energetically preferred on the bare (101) surface of anatase TiO₂ and that water molecules dissociatively adsorb on the bare (001) surface. The water adsorption on defective surfaces of TiO₂ was subsequently investigated.^{3c–e} The adsorption structures obtained in these first-principles calculations are consistent with experimental observations such as the STM measurements.^{3a} In general, submonolayer adsorption of water molecules show

attractive interaction between hydrogen in the adsorbed species (H_{adW}) and 2-fold coordinated O (O_{2c}) on the surface, which causes a local ordering.^{4,5}

In the real working conditions, however, there are intermolecular interactions between adsorbed water species and non-adsorbed water molecules above them. For this issue, first-principles calculations of bi- or trilayers of water molecules on the TiO₂ surfaces were also carried out.^{4,5} These studies suggest that the hydrogen bonds (HBs) of the H_{adW} atoms with water oxygen are rather preferable to the O_{2c} on the surface. However, the second or third layer in the multilayer calculations is already the water surface to the vacuum, and lower temperature is needed to keep water molecules unvaporized in the simulations. Therefore, it is still insufficient to evaluate subtle competition among hydrogen–oxygen interactions around the TiO₂ anatase interfaces in the aqueous environment.

In this respect, investigation of interface structures between TiO₂ surfaces and *bulk* water beyond the multilayer model system is very crucial. Though the interface between TiO₂ rutile and bulk water was investigated using a force-field method,¹¹ there has been no first-principles research on such TiO₂/bulk water interfaces until the recent report on OH adsorption on TiO₂ anatase (101)/bulk water interface.¹⁰ Thus, there are still a lot of open questions on the fundamental properties of TiO₂/bulk water interfaces. In this study, we carried out density-functional molecular dynamics simulations of TiO₂ anatase (101) and (001) surfaces dipped in bulk water (Figure 1), focusing on the adsorption manner of water molecules and the hydrogen bond (HB) network around the interface.

In the experimental side, some *in situ* experiments such as ¹H NMR and SFG spectroscopy have been recently carried out to determine the hydrogen bonds on TiO₂/water interfaces.^{8,9} The SFG spectra imply dissociative adsorption of water molecules and water molecules strongly hydrogen-bonded to the surfaces.⁹ On the other hand, on the basis of the solid-state

* To whom correspondence should be addressed. E-mail: TATEYAMA.Yoshitaka@nims.go.jp.

[†] National Institute for Materials Science (NIMS).

[‡] Japan Science and Technology Agency.

[§] Present address: Department of Physics, Tokyo University of Science, 1-3 Kagurazaka, Shinjuku, Tokyo 162-8601, Japan.

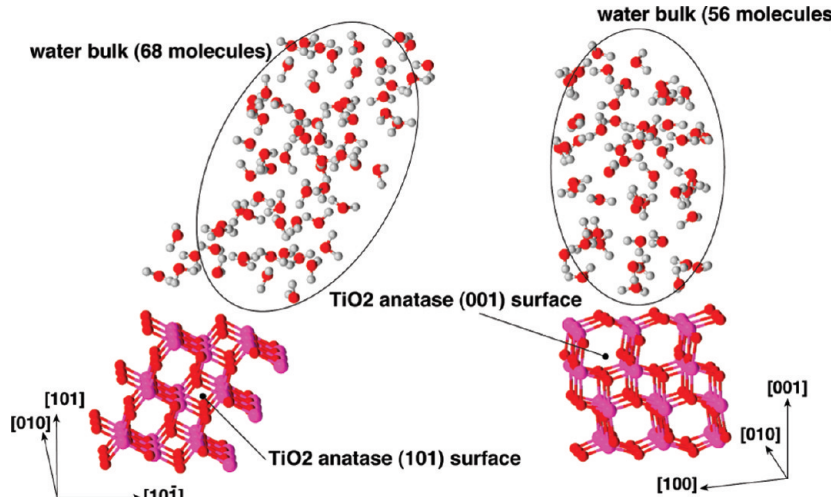


Figure 1. Schematic initial structures of TiO_2 /bulk H_2O systems. Left: anatase (101) surface/water, right: (001) surface/water.

^1H NMR spectra, Nosaka et al.⁸ classified water molecules on the anatase surface into three layers: (I) adsorbed/dissociated water most near to the surface, (II) relatively mobile water, (III) most mobile water. However, only qualitative descriptions such as *strong/weak* hydrogen bonds (HBs) were given without a clear atomistic picture. We have addressed this issue and obtained equilibrium structures (HB network) on the interface consistent with the results of solid-state ^1H NMR.⁸

To understand photocatalytic reactions¹ and photoinduced superhydrophilicity¹² in more detail, it is still necessary to answer why TiO_2 anatase (101) surfaces have high reactivity and how the OH adsorbates introduce the hydrophilicity. As described above, the bare anatase (101) surface does not seem to be so reactive according to their preference of molecular adsorption of water, whereas the bare anatase (001) surfaces have been suggested to cause water dissociation leading to the OH appearance.⁶ In fact, it is indicated that the surface of anatase nanocrystal consists of the major (101) surface with the minor (001).¹³ In this respect, comparison between these (101) and (001) surfaces is of great importance, and we have addressed this issue as well in this study.

2. Computational Details

All first-principles molecular dynamics simulations are carried out using DFT methods implemented in CPMD.¹⁴ Total energies were calculated at the Γ point in a super cell approach using BLYP generalized gradient corrected exchange-correlation functional. The Kohn–Sham orbitals were expanded by plane wave basis set up to the energy cutoff of 70 Ry. Troullier–Martin type norm-conserving pseudopotentials are used for all atoms. In particular, Ti pseudopotential utilizes the nonlinear core correction approach,¹⁵ which includes 3d and 4s in the valence electrons.

For dynamics, we use Nosé–Hoover thermostat¹⁶ with the temperature of 300 K for NVT ensemble. The time step is set to 5 au, and 500 au is used for the fictitious mass for electrons in Car–Parrinello dynamics.¹⁷ After equilibration with a couple of picoseconds (ca. 2 ps), we obtained the equilibrium trajectories, which are used to carry out sampling.

We used the (3×1) anatase (101) and (3×3) anatase (001) surfaces respectively corresponding to $(\text{TiO}_2)_{36}$ composition (Figure 1 and 2). The experimental lattice parameters¹⁸ are used. We use a monoclinic cell with the parameters of $11.3526 \times 10.2395 \times 34.0578 \text{ \AA}$ and $\alpha = 111.689$ degree for the anatase

(101)/bulk water system (left of Figure 2). The unit cell for the anatase (001)/bulk water is an orthorhombic one with the edges of $11.3526 \times 11.3526 \times 28.5438 \text{ \AA}$ (right of Figure 2). Utilizing the systems including bulk water only or each surface only, we have checked the dependence of structures on the lattice parameters, and confirmed that the experimental lattice constants give reasonable results.

Water molecules are stuffed in the open space whose size is about twice as large as that of the TiO_2 slab. Both top and bottom sides of the slab are activated as shown in Figure 2. We have checked the validity of this part of bulk water by radial distribution functions (RDF) of oxygen–oxygen (O_w – O_w) and hydrogen–hydrogen (H_w – H_w). The first peaks of $r(\text{H}_w$ – $\text{H}_w)$ and $r(\text{O}_w$ – $\text{O}_w)$ in experiment are located at 2.31 and 2.77 \AA respectively,¹⁹ whereas those of bulk water in the present systems with the (101) and (001) slabs are ca. 2.36–2.37 \AA for H_w – H_w and ca. 2.79–2.85 \AA for O_w – O_w as shown in Figure 3. It is known that BLYP exchange-correlation functional underestimates the density of liquid water.¹⁸ The BLYP value of $r(\text{O}_w$ – $\text{O}_w)$ is reported to be 2.79 \AA .²⁰ Also, our preliminary molecular dynamics simulation [$(\text{H}_2\text{O})_{100}$ in 14.41 \AA cubic cell at 297 K with the BLYP functional] of bulk water only shows the same tendency [$r(\text{H}_w$ – $\text{H}_w) = 2.34 \text{ \AA}$ and $r(\text{O}_w$ – $\text{O}_w) = 2.82 \text{ \AA}$]. Therefore, it is regarded that the water part in the present systems well describes the bulk water at the BLYP level. We have also confirmed the validity of present systems with the contour maps of the O_w density depending on water layers along the vertical axis, which is defined as the perpendicular axis to the slabs (Supporting Information).

By increasing thickness of the TiO_2 slabs and the bulk water part, we have also checked the size effect. For the anatase (101) surfaces, we examined the following systems: $(\text{TiO}_2)_{48}$ with 68 water molecules (the thickness of slab was increased) and $(\text{TiO}_2)_{36}$ with 96 water molecules (the bulk water part was increased). For the anatase (001) surfaces system, $(\text{TiO}_2)_{45}$ with 58 water molecules and $(\text{TiO}_2)_{36}$ with 85 water molecules were examined. We confirmed that there is no qualitative difference among all the systems (Supporting Information). In particular, surface structures are well described by super cells with $(\text{TiO}_2)_{36}$, as shown in the RDFs from Ti_{5c} to O on the surfaces (Figure 4). On the anatase (101) surface (part a of Figure 4), two peaks at 1.82 and 1.95 \AA in $(\text{TiO}_2)_{36}$ are also obtained in $(\text{TiO}_2)_{48}$. The peaks at 1.79 and 1.98 \AA on the anatase (001) surface (part b of Figure 4) do not depend on the slab thickness. This tendency

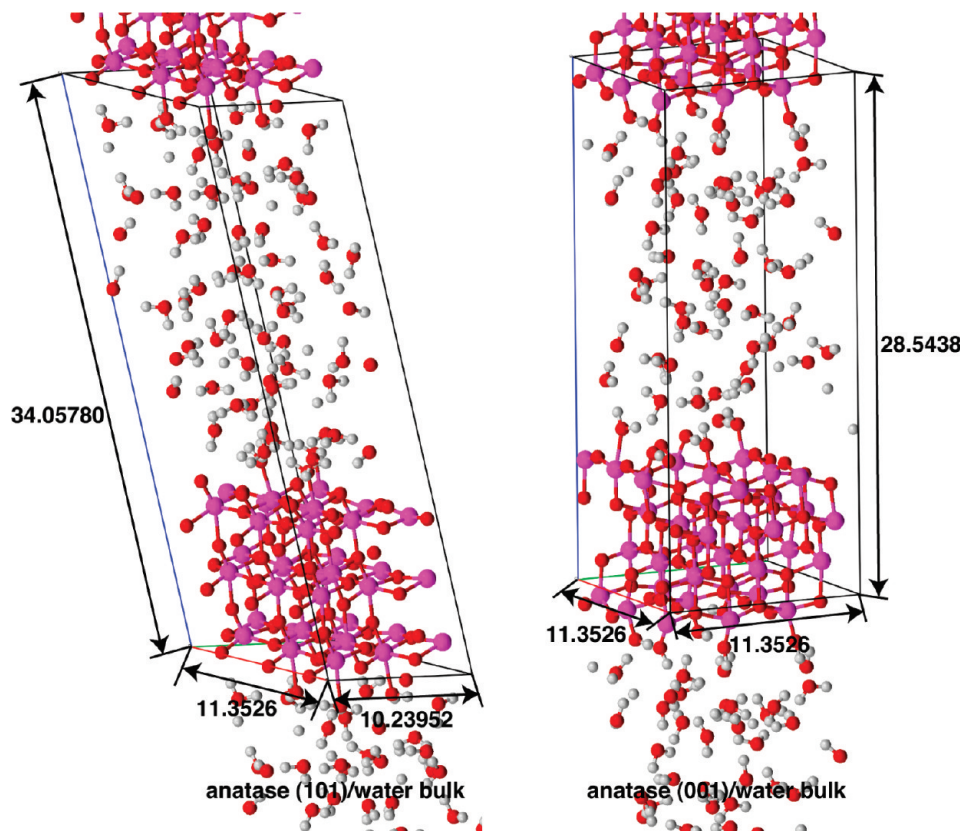


Figure 2. Unit cells we use in this work. The left one is the anatase (101) surface/water. The right is the anatase (001) surface/water. The unit of the values are in Å. The illustrated structures are snapshots in the equilibrium trajectories.

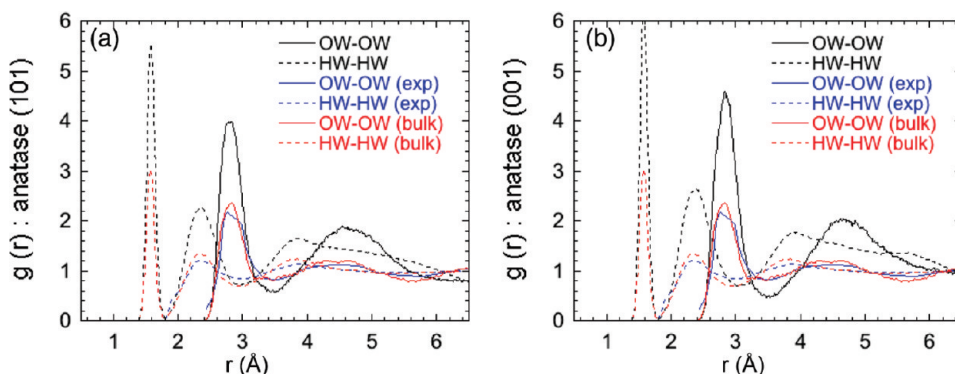


Figure 3. Radial distribution functions (RDFs) of Ow–Ow (bold lines), Hw–Hw (broken lines). Experimental results are shown by blue lines. Computational results of bulk water only are shown by red lines. The RDF of water on (a): the (101) and (b): (001) surface are shown by black lines.

does not change even if the centered Ti atoms of the $(\text{TiO}_2)_{36}$ slabs are fixed to the bulk structure (Supporting Information). This means that the character of TiO_2 anatase bulk is well reflected in the centered layer. Indeed, Ti–O bond in the centered layer of the (101) surface of $(\text{TiO}_2)_{36}$ is 1.97 Å (estimated by RDF), which is in good agreement with that of the bulk TiO_2 system in the same cell [$(\text{TiO}_2)_{108}$ system] that is, 1.98 Å. Therefore, in this study, we used the $(\text{TiO}_2)_{36}$ slabs with 68 water molecules for the anatase (101) and 56 water molecules for the anatase (001).

3. Results and Discussion

Snapshots of the equilibrium trajectories of TiO_2 anatase (101) and (001) interfaces to bulk water are shown in parts a and b respectively of Figure 5. Indices of atoms around the interfaces of $\text{TiO}_2/\text{H}_2\text{O}$ used throughout this article are schematically shown in Figure 6.

Our first-principles molecular dynamics simulations indicate that Ti_{5c} on the (101) surface, which has already been suggested to be the active sites for water adsorption,^{3–7} undergo molecular water adsorption. On the (001) surface, dissociative adsorption is predominantly observed similarly to the previous studies.⁶ For both surfaces, oxygen atoms from the water molecules (O_{adW}) bind to the Ti_{5c} on the surfaces (green oxygen atoms in Figure 5). Previous works indicate that water–water HBs are formed when there are bi- or trilayer water on the (101) surface in vacuo,^{4,5} whereas HB interaction is directed to the surface when only a few water molecules exist on the (101) surface.³ We confirmed that molecularly and dissociatively adsorbed water molecules form HBs in the direction with the bulk H_2O , not with the TiO_2 surface in a similar way to the bi- and trilayer water system.^{4,5} That is to say, adsorbed water molecules attend to the HB network of the bulk water.

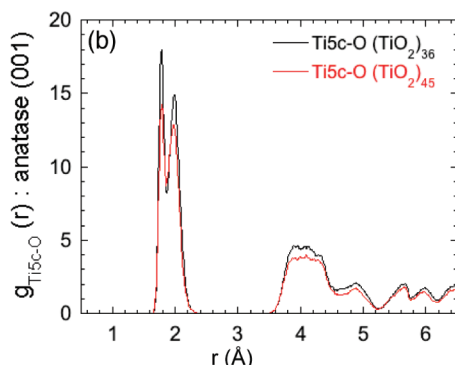
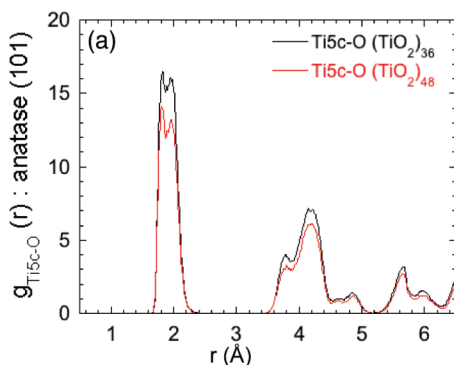


Figure 4. Radial distribution functions from $\text{Ti}_{5\text{C}}$ to oxygen atoms in the (a), anatase (101); (b), (001) surfaces. $(\text{TiO}_2)_{36}$ are shown by black lines. The results with more thick slabs of $(\text{TiO}_2)_{48}$ for anatase (101) and $(\text{TiO}_2)_{45}$ for anatase (001) are shown by red line.

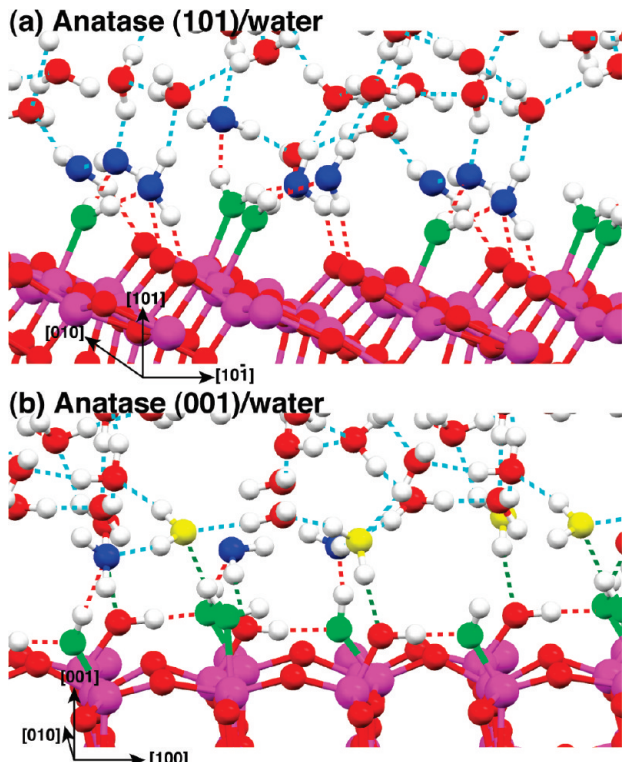


Figure 5. Snapshots of the equilibrium trajectories of the $\text{TiO}_2/\text{bulk H}_2\text{O}$ interfaces: (a) anatase (101) surface and (b) anatase (001). Water molecules or hydroxyl groups with green oxygen atoms adsorb onto five-coordinated Ti ($\text{Ti}_{5\text{C}}$). Water molecules with blue oxygen adsorb onto two-coordinated O ($\text{O}_{2\text{C}}$) or adsorbed water molecules via strong hydrogen bond (red dash lines). Waters with yellow oxygen adsorb onto H_2O or OH that are already adsorbed onto $\text{Ti}_{5\text{C}}$ via the weak hydrogen bond (green dashed lines). Cyan dashed lines show ordinary hydrogen bonds.

In addition to the qualitative agreement on this change of HB network with previous studies,^{4,5} our calculations show novel structures on the interfaces. The structure similar to the bi- or trilayer water on the (101) surface in vacuo^{4,5} is also observed (the molecular plane of adsorbed water molecules at $\text{Ti}_{5\text{C}}$ is perpendicular to [010] axis). However, we also found the water molecules adsorbed in a different way from the previous suggestion,^{4,5} that is the molecular plane of adsorbed water molecules at $\text{Ti}_{5\text{C}}$ is somewhat perpendicular to [10̄1] axis rather than [010]. This feature is clarified by the distribution of $|\phi|$ (Figure 7), which is the absolute value of the angle between the [10̄1] axis and the projected normal vector (\mathbf{n}_p) of adsorbed water molecules. The first peak at approximately 0–20° indicates the dominant existence of the water molecules whose

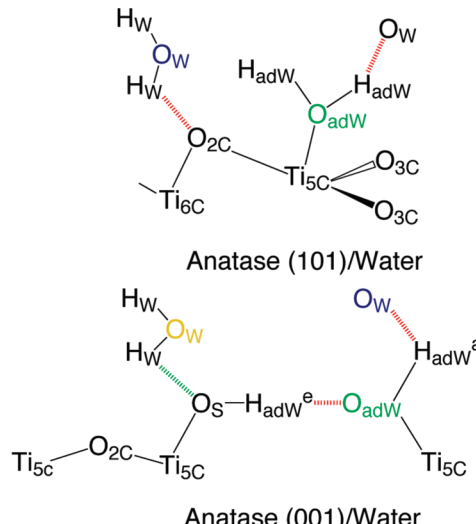


Figure 6. Indices of atoms around the interfaces of anatase (101) and (001)/water. $\text{Ti}_{5\text{C}}$: five-coordinated Ti , $\text{Ti}_{6\text{C}}$: six-coordinated Ti , $\text{O}_{2\text{C}}$: Two-coordinated O , $\text{O}_{3\text{C}}$: three-coordinated O , O_S : Origin is $\text{O}_{2\text{C}}$ on the (001) surface, O_{adW} : O of adsorbed water molecule, H_{adW} : H of adsorbed water molecule. H_{adW}^e : equatorial H of adsorbed water molecule on the (001) surface. H_{adW}^a : axial H of adsorbed water molecule on the (001) surface.

molecular plane perpendicular to the [10̄1] axis. The second peak is located around 45°. This peak indicates the existence of the adsorbed water molecule whose molecular plane is perpendicular to the [111] direction. Then, the structure similar to the bi- or trilayer water in vacuo^{4,5} corresponds to the third peak that appears at approximately 90°.

The contour maps of O_w and H_w densities along the vertical axis (Figure 8) also exhibit some structural feature. The spots of O_{adW} on the (101) surface lie just next to the $\text{Ti}_{5\text{C}}$ in the direction to [10̄1]. The spots of two hydrogen atoms (H_{adW}) attached to the O_{adW} align along the [010] direction. This indicates that the molecular plane of adsorbed water is somewhat perpendicular to [10̄1] as already mentioned. The spots of O_w in the second layer [corresponds to blue one in the Figure 5(a)], which is in the water adsorbed to $\text{O}_{2\text{C}}$ on the (101), have a more scattered distribution than O_{adW} . Consequently, we define the first layer consist of water molecules adsorbed to $\text{Ti}_{5\text{C}}$ and the second layer is constructed by the water molecules adsorbed to $\text{O}_{2\text{C}}$. The contour maps indicate that the O_w and H_w in higher layers than the second become more mobile because of their delocalized spots (see the Supporting Information).

Contour maps on the (001) surface reflect the dissociative adsorption of water molecules in a similar way to the previous

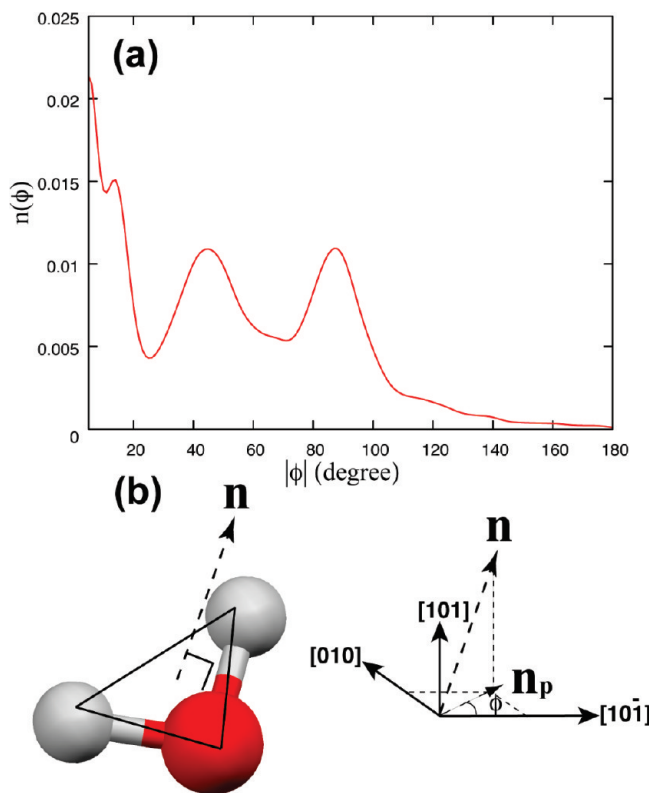


Figure 7. (a) Distribution of ϕ . Here, \square is defined as the angle between the projected normal vector (\mathbf{n}_p) of the molecular plane of adsorbed water molecules and the [101] axes. (b) Definition of the projected normal vector (\mathbf{n}_p). \mathbf{n}_p is obtained by projecting the normal vector (\mathbf{n}) of the molecule plane of adsorbed water molecule to the plane consisted of the [010] and [101] axes.

suggestion.⁶ The spots of O_{adW} on the (001) surface appear next to Ti_{5C} in the direction to [100] as shown in Figure 8. Correspondingly, the localized spots of H_{adW}^a appear just above those of O_{adW}. There are localized and delocalized spots of O_w in the second layer. The localized spots of O_w in the second layer, assigned to the blue oxygen atoms in part b of Figure 5 as will be discussed later, appear around H_{adW}^a. The delocalized wide spots of O_w of second layer, attributed to the yellow oxygen atoms in part b of Figure 5, can be assigned to the adsorbed water to the (001) surface via weak HB. The analysis by distribution functions and RDFs will show the more detailed interface structures.

Distribution profiles of O_w and H_w along the vertical direction are shown in Figure 9. According to part a of Figure 9, the peak of Ti_{5C} on the (101) surface appears around 3.77 Å and that of O_{2C} appears around 4.42 Å. The first peak of O_w, which corresponds to O_{adW}, appears around 5.80 Å and the first peak of H_w around 6.24 Å is assigned to H_{adW}. The second peak of O_w appears about 1.0 Å from its first peak. This interval between the first and second peak is very short in comparison with the position of the first peak of O_w–O_w RDF (approximately 2.85 Å). Hence, O_w in the second peak interacts with surface rather than water. More than third layer seems to become rapidly like bulk water.

The distribution profiles on the (001) surface (part b of Figure 9) shows that the peak of Ti_{5C} appears around 2.52 Å and that of O_{2C} around 3.00 Å. O_S, H_{adW}^e (the first peak of H_w), and O_{adW} (the first peak of O_w) peaks appear in the same position around 4.0 Å. This fact indicates that the O_S, H_{adW}^e, and O_{adW} lie on a plane parallel to the surface as well as the previous study⁶ (schematically shown in Figure 6). We assigned the O_w

second peak around 4.61 Å to the molecularly adsorbed H_w, the second H_w around 1.00 Å from the first peaks to H_{adW}^a, and the third H_w around 5.70 Å to molecularly adsorbed H_w.

The distribution profiles along the vertical direction are not enough to discuss the geometries in detail. Hence, we calculated the RDFs, shown in Figure 10–12 for the anatase (101) and (001) surfaces as well, to manifest the interfacial character more clearly. The important peaks of RDFs are tabulated in Table 1.

The Ti_{5C}–O_{adW} distance for the anatase (101) surface is estimated at 2.20 Å from the first peak of RDF shown in part a of Figure 10. According to the Mulliken population analysis, the charge of O_{adW} on the anatase (101) is −0.520 au, which is more electron-rich than that of O_w (Table 2). Accordingly, the polarization of the adsorbed water molecule is enhanced. Hence, the strong HB between adsorbed water species (hydrogen donor) and bulk water (hydrogen acceptor) is formed. This corresponds to the second peak of RDF of H_{adW}–O_w (part a of Figure 11) at 1.72 Å, which is shorter than that in bulk water (1.82 Å). Strong hydrogen bonds are colored by red broken line in Figure 5.

For the anatase (001), dissociative adsorption, resulting in the appearance of hydroxyl (OH) groups on the surface, is more dominant.⁶ Because two consecutive Ti_{5C} and one 2-fold oxygen atom (O_{2C}) in the direction of [100] are required for this dissociative adsorption,^{6a} one water molecule cannot dissociate when two water molecules are adsorbed at each two consecutive Ti_{5C}. The first peak of RDF of Ti_{5C}–O_w in the anatase (001)/bulk water (part b of Figure 10) is assigned to the dissociatively adsorbed water molecules, and the Ti_{5C}–O_{adW} (dissociative) distance is estimated at 1.82 Å. On the other hand, the second small one is attributed to the molecularly adsorbed water molecules, and Ti_{5C}–O_{adW} (molecularly) distance is estimated at 2.14 Å. The ratio between dissociative and molecular adsorption is 6:1 at our current calculation level.

Dissociative adsorption of water on the anatase (001) surface makes O_{adW} more electron-rich than the ordinary oxygen atoms of the bulk water (O_w). Namely, O_w is −0.458 and O_{adW} is −0.638 as shown in Table 2. Hence, O_{adW}–H_{adW}^a (as hydrogen donor) is expected to form the strong HB as hydrogen donor with water molecules (hydrogen acceptor). Indeed, according to the RDF of H_{adW}^a–O_w (part b of Figure 11), the first peak is 1.70 Å, which is shorter than 1.84 Å (the second peak of H_w–O_w), that is, the strong HB is formed. This is also reflected in the contour map of O_w in the second layer on the (001), that is, the spots of O_w just above the spots of H_{adW}^a is rather localized. In contrast to the (101) surface, molecular adsorption of water on the (001) surface does not induce significant difference between O_{adW} and O_w [O_{adW} (molecule): −0.481 O_w: −0.458]. Hence, water molecule molecularly adsorbed on the (001) surface (hydrogen donor) forms a weak HB (2.14 Å) with bulk water molecules (hydrogen acceptor).

It is noteworthy that the position of the third peak of H_{adW}^a–O_w RDF on the anatase (001) surface (4.06 Å) shown in part b of Figure 11 is significantly far off these of the H_{adW}^e–O_w and H_w–O_w (3.33–3.44 Å). This implies that the third nearest neighbor oxygen of H_{adW}^a do not make substantial HBs to bulk waters.

On the anatase (101) surface, water molecules (hydrogen donor) can also adsorb onto O_{2C} (hydrogen acceptor) via the formation of HBs as experimentally and theoretically indicated,^{4,5,7} which are shown as water molecules with blue oxygen atoms in part a of Figure 5. By comparing part a of Figure 5 with the structures in the ideal bi- and trilayer model, there are the water molecules adsorbed to O_{2C} in a similar way to those previously

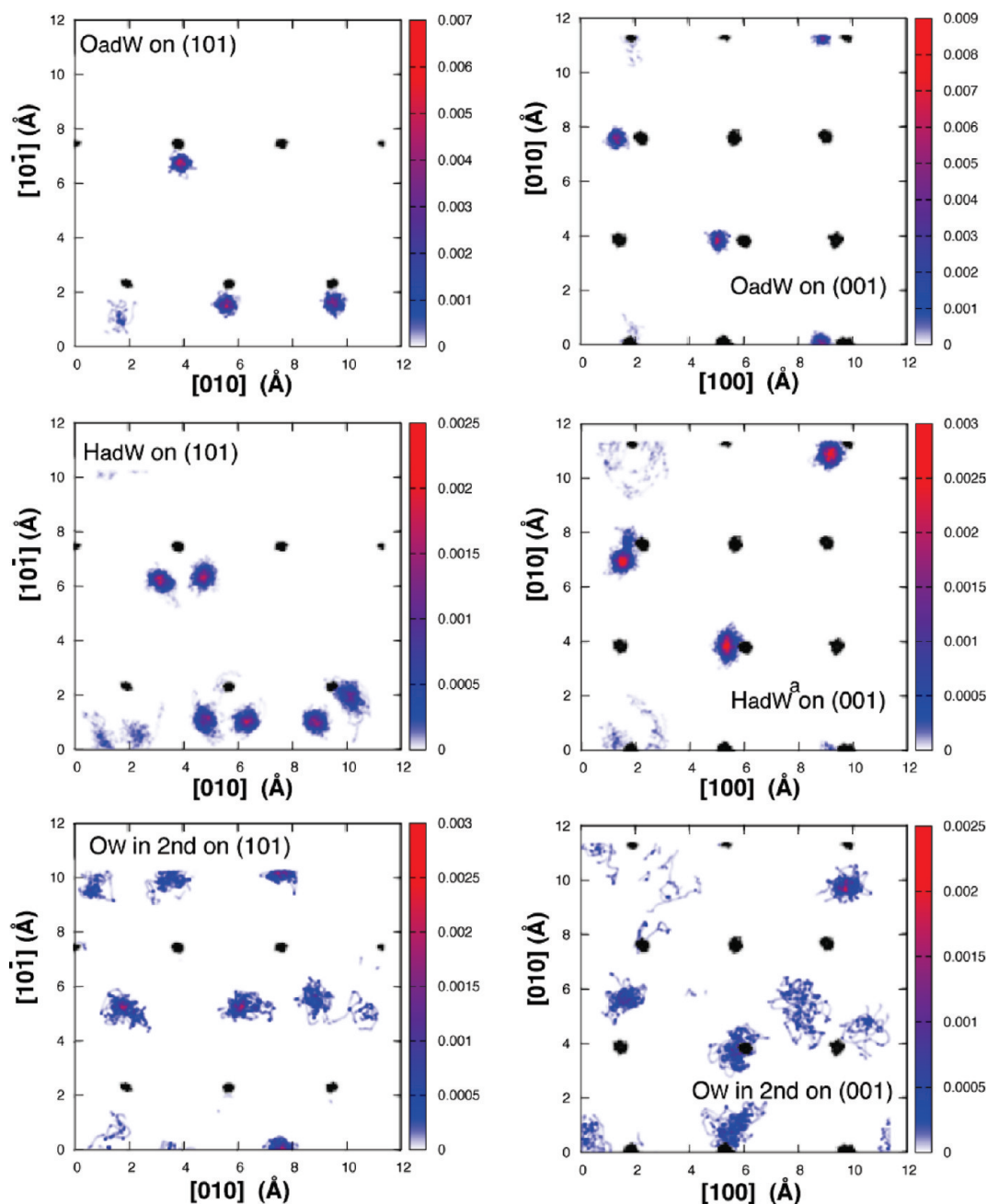


Figure 8. Contour maps of the vertical density profiles of oxygen and hydrogen atoms of water molecules in the first layer and the second. The maps in the left column are on the (101) surface. The maps in the right are on the (001) surface. Black spots indicate that the position of $\text{Ti}_{3\text{C}}$. The maps in the top are the density of O_{adw} , which are the molecularly or dissociatively adsorbed to $\text{Ti}_{3\text{C}}$. The maps in the middle are the distribution density of H_{adw} for (101) surface, and $\text{H}_{\text{adw}}^{\text{a}}$ for (001) surface. The maps in the bottom are the density of O_w of the second layer.

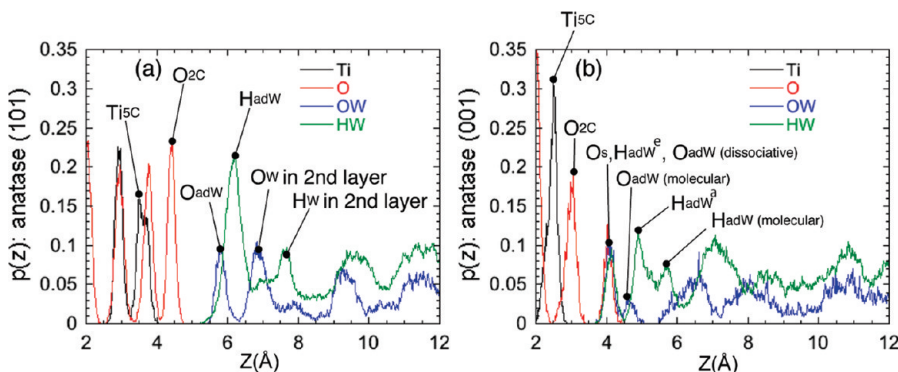


Figure 9. Density profiles along the vertical axis of Ti and O (is origin from TiO_2 surfaces) and O_w and H_w . (a) is the on the (101) surface, (b) on the (001) surface. Here, the vertical axis is defined as perpendicular axis to the TiO_2 slabs.

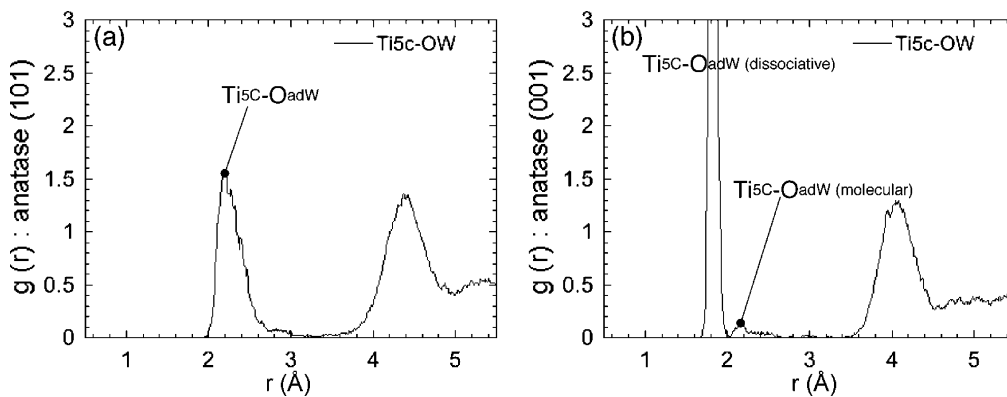


Figure 10. Radial distribution functions from Ti_{5c} to Ow: (a) is on the (101) surface, (b) is on the (001) surface.

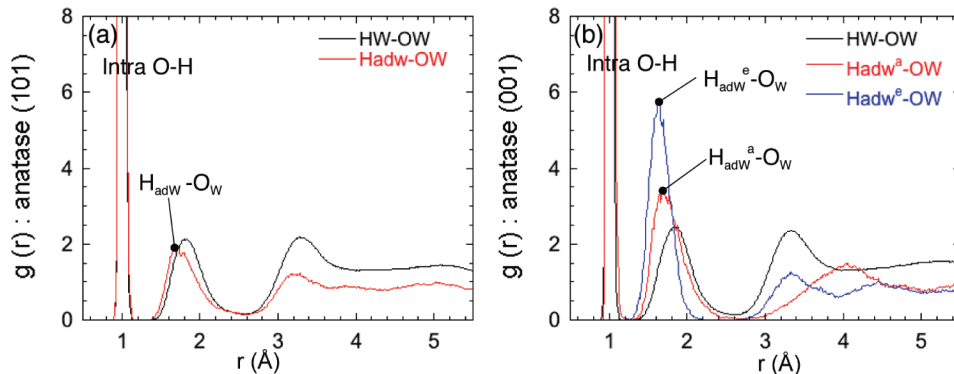


Figure 11. Radial distribution functions from Hw to Ow (black line), and from H_{adw} to Ow (red line): (a) is on the (101) surface, (b) is on the (001) surface with RDF from Hw to Ow.

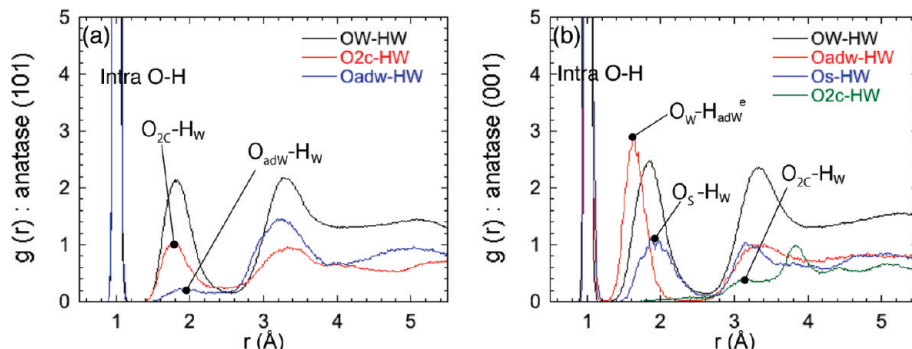


Figure 12. Radial distribution functions (RDFs) from O_{2c} [Os for (001) surfaces] to H_w with RDF from Ow to H_w.

suggested.^{4,5} However, it seems to be difficult to find the unified structural property of them except for one moiety of O—H of water molecule directed to O_{2c}. These HBs appear to be stronger than ordinary water–water HBs because the O_{2c}—H_w bond lengths are estimated at 1.78 Å on the anatase (101) compared to 1.82 Å of the O_w—H_w distance in the bulk water part, as shown in part a of Figure 12. The origin of the strong HB is attributed to the charge of O_{2c}. Mulliken population analysis shows that O_{2c} has a larger negative charge (−0.774 au on average) than Ow (−0.456 au on average). The large negative charge of O_{2c} strongly attracts hydrogen atoms.

On the anatase (001) surfaces, The first peak of RDF of O_s—H_w around 1.00 Å [here O_s indicates the originally O_{2c} on the anatase (001) surface] is attributed to the bond with H_{adw^e} withdrawn from the adsorbed water molecule. The second peak around 1.91 Å is the weak HBs with the water molecules (hydrogen donor). This is also reflected on the (001) contour map (Figure 8) of the second layer. The first peak of O_{2c}—H_w in part b of Figure 12 is around 3.14 Å. Hence, in contrast to

TABLE 1: Bond Lengths (in Å) Estimated by Radial Distribution Functions in the Anatase (101) and (001) Surface/Bulk Water Systems

bond species	length	peak
Anatase (101) Surface		
Ti _{5c} —O _{adw}	2.20	first in part a of Figure 9
H _{adw} —O _w	1.72	second in part a of Figure 10
O _{2c} —H _w	1.78	second in part a of Figure 11
H _w —O _w	1.80	second in each figures
Anatase (001) Surface		
Ti _{5c} —O _{adw} (dissociative)	1.84	first in part b of Figure 9
Ti _{5c} —O _{adw} (molecular)	2.14	second in part b of Figure 9
H _{adw^a} —O _w	1.70	second in part b of Figure 10
H _{adw^e} —O _w	1.63	second in part b of Figure 10
O _s —H _w	1.91	second in part b of Figure 11
O _{2c} —H _w	3.14	first in part b of Figure 11
H _w —O _w	1.85	second in each figure

the previous suggestion,^{6(a)} there are no water molecules adsorbed to the O_{2c}. However, the charge of the O_{2c} on the (001) (−0.810 au) is more electron-rich than that on the (101)

TABLE 2: Averaged Mulliken Charges (in au) of Atoms in the Anatase (101) and (001) Surface/Bulk Water Systems

atoms	(101)	(001)
Ti _{5C}	2.624	2.639
Ti _{6C}	2.585	2.576
O _{2C} (bridge)	-0.774	-0.810
O _S		-0.696
O _{3C}	-0.900	-0.915
O _{adW} (molecular)	-0.520	-0.481
O _{adW} (dissociate)		-0.638
O _W	-0.456	-0.458
H _{adW} (molecular)	0.317	0.341
H _{adW} (dissociate)		0.300
H _W	0.321	0.325

(-0.774 au). Therefore, it is likely that the O_{2C} on the (001) adsorbs the water molecule as hydrogen acceptor via HB. The reason for no water adsorption can be attributed to the steric repulsion.

Strong HBs on the anatase (101) surface are formed between O_{2C} (hydrogen acceptor) and H_{2O} (hydrogen donor) and between the adsorbed water (hydrogen donor) and nonadsorbed ones (hydrogen acceptor). On the anatase (001) surface, strong HB is formed between H_{adW}^e and O_{adW}, H_{adW}^a and O_W. Weak HBs are formed on the anatase (001) surface between O_S and H_W. Water molecules, which make weak HBs in the direction to the surfaces, are shown as H_{2O} molecules with yellow oxygen atoms in Figure 5.

On the basis of the above discussion, we suggested the following two-layer model. The first layer is the molecularly or dissociatively adsorbed H_{2O} to the Ti_{5C}. The definitions of the second layer are different depending on surfaces. On the (101) surfaces, the water molecules adsorbed onto O_{2C} via the formation of HBs surface are defined as the second layer. On the (001) surfaces, water molecules adsorbed to O_S and H_{adW}^a via the weak HB and strong HB can be defined as the second layer. More than third layer can be regard as bulk water.

The interface structures mentioned above are consistent with the results of solid-state ¹H NMR spectroscopy.⁸ The signal of the HB is observed in the range from 6.5 to 5.4 ppm, which is lower than that of liquid water (4.8 ppm at 298 K). This chemical shift indicates that the strong HBs are formed between the adsorbed molecules and the water aggregation. Furthermore, a higher shifted signal indicates that weak HBs are also observed depending on the photocatalyst. According to the our calculation results, this weak HBs mainly appear on the minor anatase (001) surface. Therefore, the peak intensity of solid-state ¹H NMR of the weak HBs might be useful to estimate the area of the minor (001) surface.

The consistency between the results of our simulations and those of solid-state ¹H NMR⁸ allows us to discuss the adsorption efficiency of anatase (101) and (001) surfaces. If we regard water molecules coordinated to Ti_{5C} as the adsorbed molecules, their numbers are 3.01×10^{14} and 2.72×10^{14} molecules/cm² on the anatase (101) and (001) surfaces, respectively. Thus, from the viewpoint of the number of steadily adsorbed water molecules, the anatase (101) surface is slightly superior to the anatase (001) surface.

Additionally, we carried out simulations with different initial coverages to eliminate the initial structure dependence (100% of Ti_{5C} on the surfaces are covered by water molecules). On the anatase (001) surface, we observed that intentionally adsorbed water molecules spontaneously desorb to the bulk water, indicating that the (001) surface has a critical coverage for water adsorption. Similarly, on the anatase (101) surfaces,

extra-adsorbed water molecules are desorbed to the bulk water. The one-monolayer coverage of all Ti_{5C} was not observed on both (101) and (001) surfaces at our current calculation level.

The difficulty of the one-monolayer coverage to all the Ti_{5C} sites on the (101) surface is probably due to steric repulsion. As already mentioned, water molecules adsorbed at Ti_{5C} are largely classified into three types: (I) the molecular plane of H_{2O} is perpendicular to [10̄1], (II) next one is water molecule whose molecular plane is perpendicular to [11̄1]. (III) the final one is water molecules whose molecular plane is perpendicular to [010]. According to the previous bi or trilayer models,^{4,5} if all adsorbed H_{2O} is (III) type, the full coverage seems to be possible. However, all of the types of adsorbed water molecules as shown in Figure 7 exist probably due to the entropic effect. It is difficult for water molecules to be adsorbed at all Ti_{5C} with type (I) because the steric repulsion between hydrogen atom of the water molecules.

However, the case of the (001) surface seems to depend on the cell size. The present cell of the (001) surface is 3×3 (there are three Ti_{5C} atoms along the [100] direction). Because two consecutive Ti_{5C} in the direction of [100] are required for this dissociative adsorption,^{6a} one Ti_{5C} site remains in the present (001) slab. Re-examination using a slab with even number of Ti_{5C} atom along the [100] direction (like 4×4) is needed to conclude. This problem will be an issue in the future.

Finally, we compare our results with the existing scenarios of photocatalysis¹ and superhydrophilicity.¹² We observed strong HBs on both hydrated (101) and (001) surfaces of anatase structures, although the adsorbed species are different (H_{2O} on the (101) and OH on the (001)). In this respect, the reactivity of both surfaces is likely to be similar, whereas the (101) surface has been regarded to be more reactive. Also the present results show that the hydrated surfaces already seem hydrophilic, in contrast to typical hydrophobic behavior. This may support a model of decomposition of surface contaminants. For better understanding, more intensive investigation of the hydrated surfaces should be necessary, which will be a future work.

4. Conclusions

The atomistic interface structures between TiO₂ anatase (101), (001) and bulk water are reported through the first-principles molecular dynamics calculation. Our results explicitly show the equilibrium atomistic structures on the interfaces. It is confirmed that the adsorbed water molecules make the HBs with bulk water as previously suggested.^{4,5} The first water layer can be defined as the water molecules adsorbed at Ti_{5C} on the anatase (101) and (001) surfaces molecularly or dissociatively. It is noteworthy that the molecular plane of the adsorbed waters at Ti_{5C} on the (101) surface is somewhat perpendicular to [10̄1] in contrast to the multilayer model in vacuo.^{4,5} In the first water layer, the one-monolayer coverage of all Ti_{5C} on both the (101) and (001) surface is impossible at our calculation level, that is, inactive five-coordinated Ti atoms exist on the surfaces even dipped in bulk water. The second layer on the anatase (101) surface can be defined as the water molecules adsorbed to O_{2C} or adsorbed water to Ti_{5C} via strong HB. Second layer on the (001) surface consists of water molecules, which are bound to the first layer water molecules via the strong and weak HBs. In contrast to the (101) surface, there is no water adsorbed to O_{2C}. This fact is different from the previous suggestion.⁶

As already mentioned in the introduction section, TiO₂ is widely used in many applications with an aqueous environment. Therefore, the reactivity of hydrated surfaces is important in practice. The analysis of the reactivity of the (101) and (001) surfaces are under research in our laboratory.

Acknowledgment. This work was partly supported by Grant-in-Aid for Scientific Research (C) 20540384.

Supporting Information Available: About the information of checking the cell parameters, size dependences in the TiO₂ slabs and the bulk water part, contour maps of the vertical density profiles of O_w and H_w in more than second layer, O_w–O_w radial distribution functions depending on water layers along the vertical axis, and the surface structure when centered Ti atoms of the slabs are fixed to bulk structure. This material is available free of charge via the Internet at <http://pubs.acs.org>.

References and Notes

- (1) Diebold, U. *Surf. Sci. Rep.* **2002**, *293*, 1–117. Fujishima, A.; Honda, K. *Nature* **1972**, *239*, 37–38.
- (2) Kowalski, P. M.; Meyer, B.; Marx, D. *Phys. Rev. B* **2009**, *79* (1–15), 115410. Wendt, S.; Schaub, R.; Matthiesen, J.; Vestergaard, E. K.; Wahlstrom, E.; Tasmussen, M. D.; Thostrup, P.; Molina, L. M.; Lægsgaard, E.; Stensgaard, I.; Hammer, B.; Besenbacher, F. *Surf. Sci.* **2005**, *598*, 226–245. Zhang, C.; Lindan, P. J. D. *J. Chem. Phys.* **2003**, *118*, 4620–4630. Lindan, P. J. D.; Harrison, N. M.; Holender, J. M.; Gillan, M. J. *Chem. Phys. Lett.* **1996**, *261*, 246–252.
- (3) (a) He, Y.; Tilocca, A.; Dulub, O.; Annabella, S.; Diebold, U. *Nat. Mater.* **2009**, *8*, 585–589. (b) Li, W.-K.; Gong, X.-Q.; Lu, G.; Selloni, A. *J. Phys. Chem. C* **2008**, *112*, 6594. (c) Gong, X.-Q.; Selloni, A.; Batzill, M.; Diebold, U. *Nat. Mater.* **2006**, *5*, 665–670. (d) Tilocca, A.; Selloni, A. *J. Phys. Chem. B* **2004**, *108*, 4743–4751. (e) Tilocca, A.; Selloni, A. *J. Chem. Phys.* **2003**, *119*, 7445–7450. (f) Herman, G. S.; Dohnalek, Z.; Ruzycki, N.; Diebold, U. *J. Phys. Chem. B* **2003**, *107*, 2788–2795. (g) Nakamura, R.; Imanishi, A.; Murakoshi, K.; Nakato, Y. *J. Am. Chem. Soc.* **2003**, *125*, 7443–7450.
- (4) Tilocca, A.; Selloni, A. *Langmuir* **2004**, *20*, 8379–8384.
- (5) Mattioli, G.; Filippone, F.; Caminiti, R.; Bonapasta, A. A. *J. Phys. Chem. C* **2008**, *112*, 13579–13586.
- (6) (a) Vittadini, A.; Selloni, A.; Rotzinger, F. P.; Grätzel, M. *Phys. Rev. Lett.* **1998**, *81*, 2954–2957. (b) Gong, X.-Q.; Selloni, A. *J. Phys. Chem. B* **2005**, *109*, 19560–19562. (c) Selloni, A. *Nat. Mater.* **2008**, *7*, 613–615.
- (d) Blomquist, J.; Walle, L. E.; Uvdal, P.; Borg, A.; Sandell, A. *J. Phys. Chem. C* **2008**, *112*, 16616–16621.
- (7) Herman, G. S.; Dohnalek, Z.; Ruzycki, N.; Diebold, U. *J. Phys. Chem. B* **2003**, *107*, 2788–2795.
- (8) Nosaka, A. Y.; Fujiwara, T.; Yagi, H.; Akutsu, H.; Nosaka, Y. *J. Phys. Chem. B* **2004**, *108*, 9121–9125. Nosaka, A. Y.; Nosaka, Y. *Bull. Chem. Soc. Jpn.* **2005**, *78*, 1595–1607.
- (9) Wang, C.-y.; Groenzin, H.; Shultz, M. J. *J. Am. Chem. Soc.* **2005**, *127*, 9736–9744. Uosaki, K.; Yano, T.; Nihonyanagi, S. *J. Phys. Chem. B* **2004**, *108*, 19086–19088.
- (10) Cheng, H.; Selloni, A. *Langmuir* **2010**, *26*, 11518–11525.
- (11) Pēdota, M.; Bandura, A. V.; Cummings, P. T.; Kubicki, J. D.; Wesolowski, D. J.; Chialvo, A. A.; Machesky, M. L. *J. Phys. Chem. B* **2004**, *108*, 12049–12060. Kornherr, A.; Vogtenheber, D.; Ruckenbauer, M.; Podloucky, R.; Zifferer, G. *J. Chem. Phys.* **2004**, *121*, 3722–3726. Ohler, B.; Langel, W. *J. Phys. Chem. C* **2009**, *113*, 10189–10197.
- (12) Sakai, N.; Fujishima, A.; Watanabe, T.; Hashimoto, K. *J. Phys. Chem. B* **2001**, *105*, 3023–3026. Sakai, N.; Wang, R.; Fujishima, A.; Watanabe, T.; Hashimoto, K. *Langmuir* **1998**, *14*, 5918–5920.
- (13) Diebold, U.; Ruzycki, N.; Herman, G. S.; Selloni, A. *Catal. Today* **2003**, *85*, 93.
- (14) CPMD V3.12: IBM Research division, MPI Festkoerperforschung Stuttgart: <http://www.cpmd.org>.
- (15) Louie, S. G.; Froyen, S.; Cohen, M. L. *Phys. Rev. B* **1982**, *26*, 1738.
- (16) Nosé, S. *J. Chem. Phys.* **1984**, *81*, 511. Hoover, W. G. *Phys. Rev. A* **1985**, *31*, 1695.
- (17) Car, R.; Parrinello, M. *Phys. Rev. Lett.* **1985**, *55*, 2471.
- (18) Horn, M.; Schwerdtfeger, C. F.; Meagher, E. P. Z. *Kristallogr.* **1972**, *136*, 273–281.
- (19) Soper, A. K.; Bruni, F.; Ricci, M. A. *J. Chem. Phys.* **1997**, *106*, 247–254.
- (20) Todrova, T.; Seitsonen, A. P.; Hutter, J.; Kuo, I.-F. W.; Mundy, C. J. *J. Phys. Chem. B* **2006**, *110*, 3685–3691. Kuo, I.-F. W.; Mundy, C. J.; MacGrath, M. J.; Siepmann, J. I.; Vondele, J. V.; Sprik, M.; Hutter, J.; Chen, B.; Klein, M. L.; Mohamed, F.; Krack, M.; Parrinello, M. *J. Phys. Chem. B* **2004**, *108*, 12990–12998. Grossman, C. J.; Schwegler, E.; Draeger, E. W.; Gygi, F.; Galli, G. *J. Chem. Phys.* **2004**, *120*, 300–311.

JP105364Z